



ANISOTROPY CHARACTERIZATION OF I-125 SEED WITH ATTACHED ENCAPSULATED COBALT CHLORIDE COMPLEX CONTRAST AGENT MARKERS FOR MRI-BASED PROSTATE BRACHYOTHERAPY

STEVEN J. FRANK, M.D., RAMESH C. TAILOR, PH.D., RAJAT J. KUDCHADKER, PH.D.,
 KAREN S. MARTIROSYAN, PH.D., R. JASON STAFFORD, PH.D., ANDREW M. ELLIOTT, PH.D.,
 DAVID A. SWANSON, M.D., DAVID SING, B.S., JONATHAN CHOI, B.S.,
 FIRAS MOURTADA, PH.D., and GEOFFREY S. IBBOTT, PH.D.

Departments of Radiation Oncology, Radiation Physics, Imaging Physics, and Urology, The University of Texas M. D. Anderson Cancer Center, Houston, TX; and Department of Chemical and Biomolecular Engineering, The University of Houston, Houston, TX

(Received 23 September 2009; accepted 9 March 2010)

Abstract—We have developed a novel MRI marker for prostate brachytherapy. The purpose of this study was to evaluate the changes in anisotropy when cobalt chloride complex contrast agent encapsulated contrast agent markers (C4-ECAM) were placed adjacent to an iodine-125 (I-125) titanium seed, and to verify that the C4-ECAMs were visible on magnetic resonance imaging (MRI) after radiation exposure. Two C4-ECAMs were verified to be MRI visible in a phantom before radiation exposure. The C4-ECAMs were then attached to each end of a 12.7-U (10-mCi) I-125 titanium seed in a polymer tube. Anisotropy was measured and analyzed with the seed alone and with attached C4-ECAMs by suspending thermoluminescent dosimeters in a water phantom in 2 circles surrounding the radioactive source with radius of 1 or 2 cm. A T1-weighted MRI evaluation of C4-ECAMs was then performed after exposure to the amount of radiation typically delivered during 1 month of prostate brachytherapy. Measured values of the anisotropy function $F(r, \theta)$ for the I-125 seed with and without the C4-ECAMs were mutually statistically indistinguishable (standard error of the mean $<4.2\%$) and agreed well with published TG-43 values for the bare seed. As expected, the anisotropy function $\phi_{an}(r)$ for the 2 datasets (with and without C4-ECAMs) derived from the measured $F(r, \theta)$ did not exhibit statistically measurable difference. Both datasets showed agreement with the published TG-43 $\phi_{an}(r)$ for the bare seed. The C4-ECAMs were well visualized by MRI after 1 month of radiation exposure. There were no changes in anisotropy when the C4-ECAMs were placed next to an I-125 radioactive seed, and the C4-ECAMs were visualized after radiation exposure. © 2010 American Association of Medical Dosimetrists.

Key Words: MRI-based dosimetry, Fiducial marker, Post-implant dosimetry, Prostate brachytherapy.

INTRODUCTION

Prostate brachytherapy is a minimally invasive standard-of-care approach for the treatment of prostate cancer.¹ Outcomes with high-quality prostate brachytherapy implants are good, but there is substantial heterogeneity in implant quality among radiation oncologists.² Standard imaging modalities such as ultrasonography, fluoroscopy, and computed tomography (CT) that are currently used during treatment planning, treatment delivery, and postimplant treatment quality evaluations provide inferior visualization of the prostate and surrounding critical organ structures, which leads to subjective determination of the quality of treatment.

In contrast, magnetic resonance imaging (MRI) provides superior visualization of the soft tissues of the prostate gland and surrounding normal critical struc-

tures.³ However, with MRI, the radioactive iodine seeds and spacers used for prostate brachytherapy and the needle tracks resulting from the implant procedure appear as negative contrast voids on the images, meaning that the iodine seeds cannot be accurately localized within the prostate and periprostatic tissue.^{4,5} Because of this problem, MRI-based dosimetry is not routinely used in prostate brachytherapy. To facilitate MRI-based dosimetry, we have recently developed an encapsulated contrast agent marker (ECAM) comprised of a cobalt chloride complex contrast agent (C4) that facilitates the positive identification of the implanted radioactive seeds under MRI.^{5,6} To permit positive identification of the titanium seeds under MRI, the C4-ECAMs are placed directly adjacent to the radioactive seeds at their distal ends (Fig. 1).

Over the last decade, we have implanted iodine-125 (I-125) source in over 98% of our prostate cancer patients treated with brachytherapy. I-125 emits gamma rays, or photons, with a maximum energy of 35 keV, and a photon's energy can be absorbed by an atom's loosely bound planetary electrons. An electron that absorbs a

Presented at the American Brachytherapy Society Annual Meeting, Toronto, Canada, May 31–June 2, 2009.

Reprint requests to: Steven J. Frank, M.D., Department of Radiation Oncology, Box 97, The University of Texas M. D. Anderson Cancer Center, 1515 Holcombe Blvd, Houston, TX 77030. E-mail: sjfrank@mdanderson.org

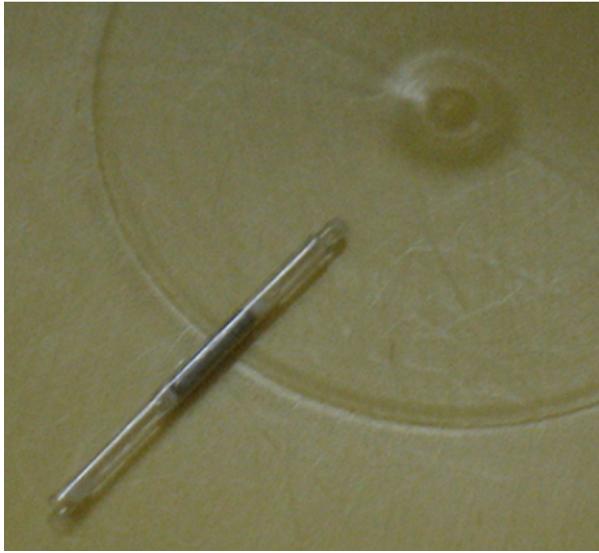


Fig. 1. C4-ECAMs placed adjacent to the titanium radioactive seed for dosimetric analysis.

photon's energy is subsequently ejected from its atom and, after its interaction with a water molecule (H_2O), produces a hydroxyl radical ($OH\cdot$). In radiation therapy, these hydroxyl radicals play an important role in inducing damage to the DNA of tumor cells, resulting in cell death. The image obtained from MRI is directly related to the proton (H^+) relaxation times after induction of a magnetic field, and the effect of the hydroxyl radicals produced by radiation exposure on the amorphous-like structure of C4, and thus on the ability of C4 to maintain a positive T1 signal, is unknown. If our C4-ECAM is to be successfully used for MRI-based dosimetry, the ECAM must not alter the anisotropy and should retain its positive T1 signal under MRI after irradiation.

The purpose of this study was to determine if C4-ECAMs placed adjacent to a standard titanium I-125 radioactive seed would affect anisotropy and to determine whether C4 would maintain its positive T1 signal under MRI after the equivalent of 1 month of radiation exposure.

METHODS AND MATERIALS

Fabrication of C4-ECAMs and integration with the radioactive titanium seed

Extruded polycarbonate microtubing (outer diameter = 0.8 mm and inner diameter = 0.5 mm) was used as a robust material for encapsulation of C4 contrast agent. The microtubing was cut into 5.5-mm sections. A tiny polymer plug was fastened to one end of each 5.5-mm tube and was secured in place by local heating. C4 was then injected into the tube using a high-pressure stainless steel syringe. A second polymer plug was then fastened to the remaining end of the tube, and again, the plug was

secured in place by local heating to prevent any leakage of the contrast agent.

To fabricate the radioactive seed-ECAM unit, we used flexible and biodegradable polyglycolic acid tubing (IsoStrand, CP Medical, Portland, OR). This standard tubing had an internal diameter of 0.9 mm, which meant that the radioactive titanium seeds and fabricated C4-ECAMs could be passed into the tubing.

Measurement of 2D anisotropy function

We used the American Association of Physicists in Medicine TG-43 and TG-43U1 protocols for dose calculation around brachytherapy sources^{7,8}:

$$\dot{D}(r, \theta) = S_K \bullet \Lambda \bullet \frac{G_L(r, \theta)}{G_L(r_0, \theta_0)} \bullet g_L(r) \bullet F(r, \theta), \quad (1)$$

where Λ is the dose rate constant, S_K is the air kerma strength, $G_L(r, \theta)$ is the source geometry function, $g_L(r)$ is the radial dose function, and $F(r, \theta)$ is the two-dimensional (2D) anisotropy function. The 2D anisotropy function describes the variation in the dose rate caused by attenuation by the source encapsulation as a function of polar angle relative to the transverse plane. The 2D anisotropy function $F(r, \theta)$ is defined as:

$$F(r, \theta) = \frac{\dot{D}(r, \theta) G_L(r, \theta_0)}{\dot{D}(r, \theta_0) G_L(r, \theta)}. \quad (2)$$

Although $F(r, \theta)$ on the transverse plane is defined as unity, the value of $F(r, \theta)$ off the transverse plane typically decreases as r decreases and as θ approaches 0° or 180° .

A 12.7-U (10-mCi) I-125 seed (model 6711; GE Healthcare-Oncura, Arlington Heights, IL) was purchased specifically for this study. The I-125 seed was independently calibrated at The University of Texas M. D. Anderson Cancer Center's accredited dosimetry calibration laboratory. Thermoluminescent dosimeter (TLD) capsules, which are often used for measurements of dosimetric parameters were used in this study. The I-125 seed-ECAM unit was attached to a post as shown in Fig. 2. $F(r, \theta)$ was measured employing a jig as previously described.⁹ The jig allowed positioning of the TLD capsules around the radioactive seed-ECAM unit in concentric circles with radius (r) of 1 or 2 cm (Fig. 3). Each circle held a set of 24 TLD capsules at 15-degree intervals. Measurements were made with just one circle of TLDs ($r = 1$ or 2 cm) in place at a time to prevent possible interference from TLD capsules in the other circle because of the difference in attenuation between water and TLD capsules. Because the TLD capsules were 7 mm long, the TLD powder integrated dose over a range of polar angles (θ). The effective angle of measurement was determined by numerical analysis (Fig. 4) and is reflected in the results. For the TLD positioned at $\theta = 0^\circ$, the effective angle was 9.6° for $r = 1$ cm and 5.0°

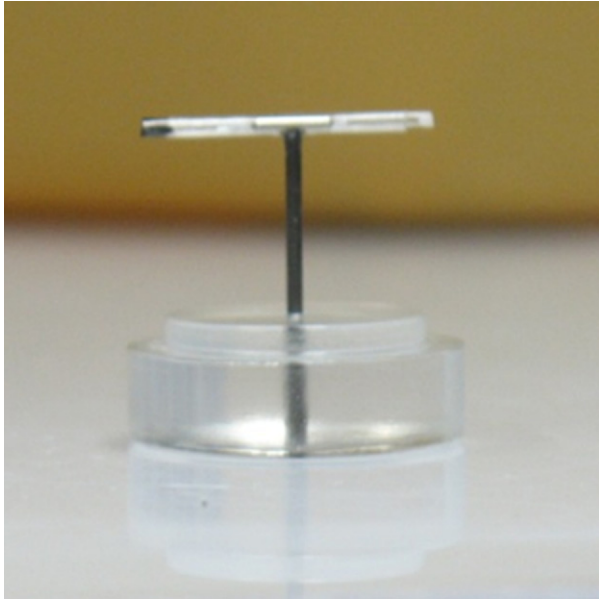


Fig. 2. I-125 seed-ECAM unit attached to a post. This system was placed inside the water phantom for dosimetric analysis.

for $r = 2$ cm. All the measurements were performed and the TLDs were read at the M. D. Anderson Cancer Center Radiological Physics Center. Each set of measurements was repeated for verification purposes. For each radial distance ($r = 1$ or 2 cm), measurements were performed with the model-6711 I-125 seed, both without and with attached C4-ECAMs. For comparative analysis, all data were normalized at 90° . For all data, the percentage standard error of the mean, which is the standard deviation divided by the square root of the number of measurements, was determined.

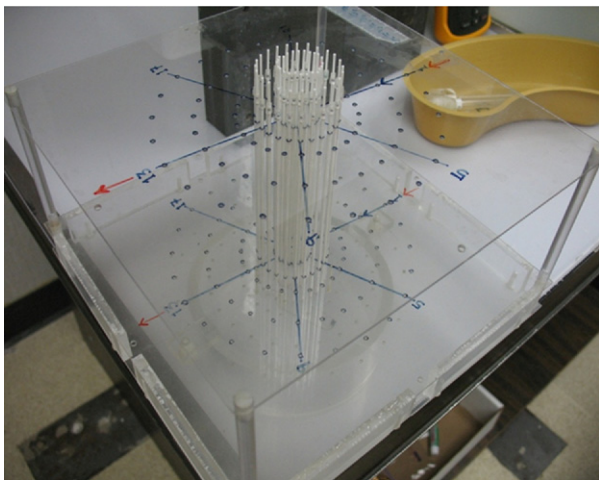


Fig. 3. The TLD capsules were positioned in a jig in concentric circles with radius of 1 or 2 cm around the I-125 seed-ECAM unit.

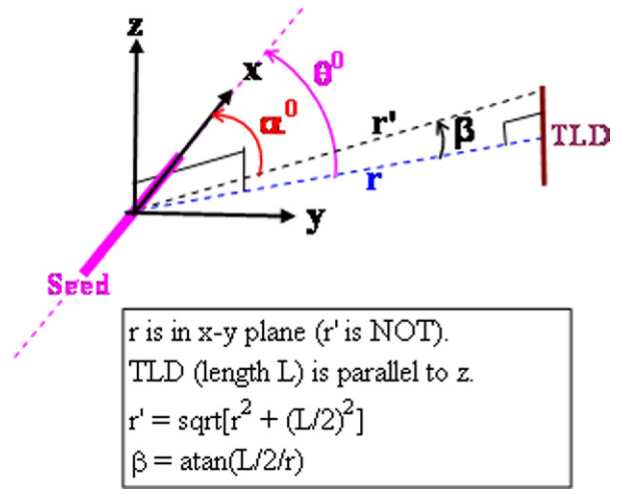


Fig. 4. The center of a TLD capsule (length “L” = 7 mm) is shown at a relative position (r , θ) with respect to the seed center. Angle “ α ” made by the tip of TLD with respect to the seed-axis is determined from the geometry shown here.

The 2D anisotropy function was calculated from the dose measurements after a procedure prescribed by Rivard *et al.*⁷ Equations (9) and (12) from the American Association of Physicists in Medicine TG-43 protocol were combined to obtain the following equation, and values for $\phi_{an}(r)$ were numerically calculated from the measured $F(r, \theta)$ ⁸:

$$\phi(r) = \sum \left[\frac{G(r, \theta)}{G(r, \theta_0)} \bullet F(r, \theta) \bullet \sin(\theta) \Delta\theta \right],$$

$$\theta = 0 \quad \text{to} \quad \frac{\pi}{2}. \quad (3)$$

The technique was verified by reproducing TG-43 reported $\phi(r)$ values from the TG-43 $F(r, \theta)$ values.⁷

ECAM visibility after the equivalent of 1 month of radiation exposure

To determine whether C4 would maintain its positive T1 signal after the equivalent of 1 month of radiation exposure, the C4-ECAMs were placed in a “gel” phantom made of 1.5% agarose powder and water. A T1-weighted MRI scan was performed before and after a 30-day radiation dose equivalent to the cumulative dose that would be received over a typical month of prostate brachytherapy. A series of images was acquired using clinical prostate MRI sequencing protocols (T1- and T2-weighted fast spin echo) on a 1.5-T MRI scanner (Signa; GE Medical Systems, Waukesha, WI), as well as high-resolution 3D axial T1-weighted fast spoiled gradient echo protocol (TR/TE = 5 ms/1.5 ms, matrix = 256×256 , receiver bandwidth = 240 Hz/pixel, FOV = $18 \text{ cm} \times 18 \text{ cm}$, slice thickness = 2 mm skip – 1 mm [interpolated], 5 averages).

Table 1. Anisotropy function $F(r, \theta)$ for the I-125 seed with and without C4-ECAMs

$r = 1 \text{ cm}$							
θ degree:	9.6	19.6	32.6	46.6	60.9	75.4	90.0
$F(r, \theta)$ without C4	0.419	0.585	0.785	0.889	0.961	0.988	1.000
$F(r, \theta)$ with C4	0.429	0.617	0.831	0.976	1.018	0.988	1.000
$r = 2.0 \text{ cm}$							
θ degree:	5.0	16.5	30.7	45.4	60.2	75.1	90.0
$F(r, \theta)$ without C4	0.456	0.634	0.820	0.895	0.970	1.022	1.000
$F(r, \theta)$ with C4	0.489	0.657	0.844	0.955	1.013	1.040	1.000

RESULTS

The measured data for the I-125 seed without an adjacent marker were consistent with previously published data.⁷ Placement of the C4-ECAMs adjacent to the I-125 radioactive seed had no measurable effect on the seed anisotropy for distances ≥ 1 cm from the seed's center. Within our measurement uncertainty (standard error of the mean $< 4.7\%$), the measured values of 2D anisotropy function $F(r, \theta)$ for the I-125 seed with and without C4-ECAMs were equivalent, as shown in Table 1.

These measured $F(r, \theta)$ values are graphically presented in Figs. 5 and 6. The two datasets (with and without C4 markers) were not statistically different. The datasets were also consistent with the TG-43 data, which are included in Figs. 5 and 6. As expected, one-dimensional anisotropy $\phi_{an}(r)$ values determined from these data were equivalent with and without C4-ECAMs (0.913 without *versus* 0.951 with C4 at $r = 1$ cm, and 0.927 without *versus* 0.958 with C4 at $r = 2$ cm). The largest discrepancy, 4.2% for $r = 1$ cm, was within the uncertainty of measurements. The published (TG-43) $\phi_{an}(r)$ values are 0.944 for $r = 1$ cm and 0.941 for $r = 2$ cm.

The values for the I-125 seed obtained from the TG-43 update were compared with our results.⁶ There

was no significant difference between the anisotropy with or without the C4-ECAMs and the anisotropy in the TG-43 dataset, and they were within measurement uncertainty ($\pm 2\sigma$) including at least 95% of all data. The values for $\theta(r)$ derived from the measured $F(r, \theta)$ agreed with the published values.⁵ The largest difference was 3% for the $r = 1$ cm dataset and 1.8% for the $r = 2$ cm dataset.

The C4-ECAMs were removed from their location adjacent to the radioactive seed, placed within a "gel" phantom, and following our standard clinical MR protocols, maintained a positive contrast signal on T1-weighted sequencing after the equivalent of 1 month of radiation exposure (Fig. 7).

DISCUSSION

Our findings show that placement of C4-ECAMs adjacent to a standard radioactive I-125 seed used for prostate brachytherapy does not alter the standard anisotropy function. Furthermore, after exposure to the amount of radiation typically delivered during 1 month of prostate brachytherapy, the C4-ECAMs maintained a positive T1-weighted MRI signal. The significance of these findings is that we can now facilitate MRI-based dosimetry by positively identifying the location of im-

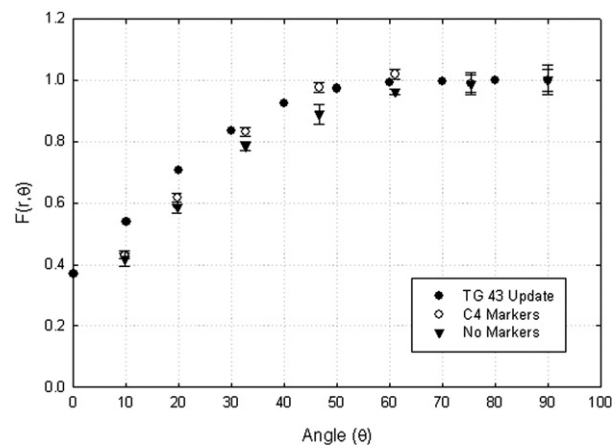


Fig. 5. The measured anisotropy function $F(r, \theta)$ for $r = 1$ cm without and with attached C4-ECAMs. Published values for the seed without marker are also shown in solid black circles for comparison.⁵ All data show good mutual agreement within the measurement uncertainties.

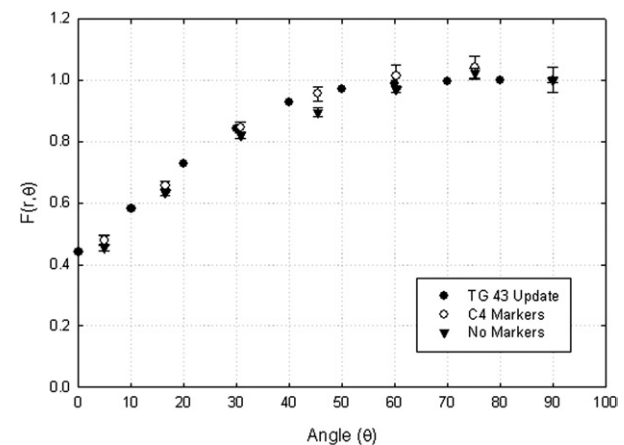


Fig. 6. The measured anisotropy function $F(r, \theta)$ for $r = 2$ cm without and with attached C4-ECAMs. Published values for the seed without marker are also shown in solid black circles for comparison.⁵ All data show good mutual agreement within the measurement uncertainties.

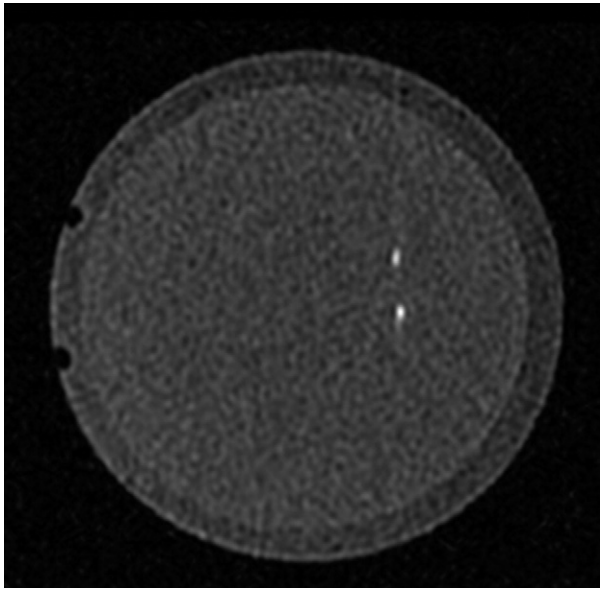


Fig. 7. After a simulated 30-day radiation exposure, the two C4-ECAMs were still visible on T1-weighted MRI.

planted radioactive titanium seeds using C4-ECAMs. In the future, MRI-based dosimetry may be able to replace CT-based dosimetry as the standard-of-care quality assurance evaluation after prostate brachytherapy.

After prostate brachytherapy, clinicians are able to use MRI to identify the base, the lateral margins, and the apex of the prostate gland. With precise localization of the implanted radioactive seeds, MRI-based dosimetry would permit a more precise evaluation of the radiation dose to the prostate cancer within the prostate gland. If MRI-based dosimetry revealed that the prostate cancer was not being adequately treated, the patient could be taken back to the operating room and additional seeds could be implanted to optimize treatment and ensure the highest probability of cancer cure. Furthermore, MRI-based dosimetry might improve patients' quality of life after brachytherapy because MRI gives clinicians additional anatomical information not available with standard imaging modalities and therefore allows clinicians to develop a more comprehensive appreciation of the dosimetric implications of treatment delivery and technique. Specifically, critical normal structures can be identified using MRI but not CT in the postimplant setting, including the internal and external urinary sphincters, neurovascular bundles, ejaculatory ducts, and anterior wall of the rectum.

Like other institutions, our institution has considered MRI-CT fusion in the postimplant setting to optimize quality.^{10,11} However, we have not been satisfied with MRI-CT fusion because of the added expense, inconvenience, and lack of anatomical and technical precision of the fused images and subsequent dosimetry. The lack of anatomical precision is due to differences in bladder and rectal filling at the times of the MRI and CT

studies. The lack of technical precision can be attributed to the differences in the table tops for the imaging units and the precise slice configuration. Novel MRI protocol sequences have been used in an attempt to optimize the location of the titanium seeds, but up to 8.5% of seeds may still not be detected with such sequences.¹² In a treatment with millimeter precision to optimize the therapeutic ratio, precise seed localization with soft-tissue anatomical information may be achieved with C4-ECAMs.

After our initial proof-of-concept study,⁵ this study provides further evidence that MRI-based dosimetry using MRI markers is feasible. Although other investigators have demonstrated *real-time* intraoperative MRI-guided prostate brachytherapy,¹³ C4-ECAMs could facilitate MRI-based dosimetry with more accurate localization of the implanted radioactive seeds. Furthermore, with use of C4-ECAMs, MRI may be able to replace ultrasonography, CT, and fluoroscopy as the standard-of-care imaging modalities for treatment planning, treatment delivery, and postimplant treatment quality evaluation for prostate brachytherapy.

In conclusion, C4-ECAMs may be used to facilitate MRI-based prostate brachytherapy by precisely localizing the implanted radioactive seeds without altering the radiation treatment. We are currently performing Monte Carlo calculations to provide an accurate model of the dosimetric implications, including the radial dose function and dose-rate constant impact of C4-ECAMs for phantom and *in vivo* canine studies.

Acknowledgments—We wish to thank the Prostate Cancer Foundation for grant support of this research, and Stephanie Deming for editing the manuscript.

REFERENCES

1. NCCN Clinical Practice Guidelines in Oncology. Home page. 2009. Available at: <http://www.nccn.org>. Accessed September 1, 2009.
2. Merrick, G.S.; Butler, W.M.; Wallner, K.E.; *et al.* Variability of prostate brachytherapy pre-implant dosimetry: A multi-institutional analysis. *Brachytherapy*. **4**:241–51; 2005.
3. McLaughlin, P.W.; Troyer, S.; Berri, S.; *et al.* Functional anatomy of the prostate: Implications for treatment planning. *Int. J. Radiat. Oncol. Biol. Phys.* **63**:479–91; 2005.
4. Nag, S.; Bice, W.; DeWyngaert, K.; *et al.* The American Brachytherapy Society recommendations for permanent prostate brachytherapy postimplant dosimetric analysis. *Int. J. Radiat. Oncol. Biol. Phys.* **46**:221–30; 2000.
5. Frank, S.J.; Stafford, R.J.; Bankson, J.A.; *et al.* A novel MRI marker for prostate brachytherapy. *Int. J. Radiat. Oncol. Biol. Phys.* **71**:5–8; 2008.
6. Martirosyan, K.S.; Stafford, R.J.; Elliott, A.M.; *et al.* PMMA/SWCNTs composites for prostate brachytherapy MRI contrast agent markers. *NSTI-NanoTech.* **2**:44–7; 2009.
7. Rivard, M.J.; Coursey, B.M.; DeWerd, L.A.; *et al.* Update of AAPM Task Group No. 43 report: A revised AAPM protocol for brachytherapy dose calculations. *Med. Phys.* **31**:633–74; 2004.
8. Nath, R.; Anderson, L.L.; Luxton, G.; *et al.* Dosimetry of interstitial brachytherapy sources: Recommendations of the AAPM Radiation Therapy Committee Task Group No. 43. *Med. Phys.* **22**: 209–34; 1995.

9. Tailor, R.; Tolani, N.; Ibbott, G.S. Thermoluminescence dosimetry measurements of brachytherapy sources in liquid water. *Med. Phys.* **35**:4063–9; 2008.
10. Servois, V.; Chauveinc, L.; El Khoury, C.; *et al.* [CT and MR image fusion using two different methods after prostate brachytherapy: Impact on postimplantation dosimetric assessment] [French]. *Cancer. Radiother.* **7**:9–16; 2003.
11. Amdur, R.J.; Gladstone, D.; Leopold, K.A.; *et al.* Prostate seed implant quality assessment using MR and CT image fusion. *Int. J. Radiat. Oncol. Biol. Phys.* **43**:67–72; 1999.
12. Bloch, B.N.; Lenkinski, R.E.; Helbich, T.H.; *et al.* Prostate post-brachytherapy seed distribution: Comparison of high-resolution, contrast-enhanced, T1- and T2-weighted endorectal magnetic resonance imaging versus computed tomography: Initial experience. *Int. J. Radiat. Oncol. Biol. Phys.* **69**:70–8; 2007.
13. D'Amico, A.V.; Cormack, R.; Tempny, C.M.; *et al.* Real-time magnetic resonance imaging-guided interstitial brachytherapy in the treatment of select patients with clinically localized prostate cancer. *Int. J. Radiat. Oncol. Biol. Phys.* **42**:507–15; 1998.